

22p

N63-10369

CODE U

NASA TN D-1447

NASA TN D-1447



TECHNICAL NOTE

D-1447

THE MAGNETIC FIELD OF A MODEL RADIATION BELT NUMERICALLY COMPUTED

Syun-Ichi Akasofu
University of Alaska
College, Alaska

Joseph C. Cain
Goddard Space Flight Center
Greenbelt, Maryland

Sydney Chapman
University of Alaska
College, Alaska

NATIONAL AERONAUTICS AND SPACE ADMINISTRATION

WASHINGTON

November 1962

THE MAGNETIC FIELD OF A MODEL RADIATION BELT NUMERICALLY COMPUTED

by

Syun-Ichi Akasofu
University of Alaska

Joseph C. Cain
Goddard Space Flight Center

Sydney Chapman
University of Alaska

SUMMARY

The magnetic field of a ring-current belt symmetrically encircling the earth is calculated numerically, to a first approximation, for a particular model belt discussed elsewhere by Akasofu and Chapman. They calculated the first approximation to the field only for points in the equatorial plane. The whole distribution of the field is discussed here, and for a particular intensity of the belt the calculation is carried to a second approximation. The field of the ring current is shown to be nearly uniform over the earth's surface, although the diamagnetism of the belt produces an insignificant irregularity in the field disturbance in auroral latitudes. In the model belt considered here is one whose center line is connected with the auroral zone by the dipole field lines of force. Although its particles have not yet been observed directly, its existence is suggested by the quiet day anomaly of the satellite-observed magnetic field at six earth radii. The known Van Allen radiation belts probably contribute little to the ring current field, but during magnetic storms the radius of the belt mainly responsible for this field is probably less than this distance.

CONTENTS

Summary	i
INTRODUCTION.	1
GEOMETRICAL CONSIDERATIONS.	2
THE MODEL RADIATION BELT	4
THE CURRENT DISTRIBUTION CORRESPONDING TO $\Delta_1 F$	6
THE MAGNETIC FIELD $\Delta_1 F$	7
THE RING-CURRENT MAGNETIC DISTURBANCE OF THE EARTH'S SURFACE FIELD	13
THE SECOND APPROXIMATION ($\Delta_2 F$) TO THE FIELD OF THE RING CURRENT	14
THE RING-CURRENT FIELD BEYOND THE BELT	16
THE NONSTEADY STATE.	17
ADDENDUM	17
References	18

THE MAGNETIC FIELD OF A MODEL RADIATION BELT NUMERICALLY COMPUTED *

by

Syun-Ichi Akasofu
University of Alaska

Joseph C. Cain
Goddard Space Flight Center

Sydney Chapman†
University of Alaska

INTRODUCTION

Space observations by Van Allen and Frank (Reference 1) and by Vernov, Chudakov, et al. (Reference 2) have shown that the earth is encircled by radiation belts which are composed of charged particles trapped in the magnetic field F in the space around the earth (Reference 3).

A group of particles trapped in the earth's magnetic field produces a magnetic field ΔF by their motions in this field. The total field vector H is the vector sum of the intensities H_E and ΔH of the earth's magnetic field F_E and the field ΔF of the belt; thus

$$H = H_E + \Delta H, \quad (1)$$

which may be expressed symbolically by

$$F = F_E + \Delta F. \quad (2)$$

The total field F and the precise distribution of the particles in the belt are interconnected in a somewhat complex way. Successive approximation provides one method of investigating this relationship. To apply this method to a model belt whose particle content and general distribution are known or "assumed", the following steps are taken:

1. Calculate the particle distribution and the magnetic field of the belt as if the total field present were simply the earth's field F_E . Let the belt field thus calculated be denoted by $\Delta_1 F$. Let the field $F_E + \Delta_1 F$ be denoted by F_1 .
2. Calculate the particle distribution and the magnetic field of the belt as if the total field present were F_1 . Let the belt field thus calculated be denoted by $\Delta_2 F$, and let F_2 denote the field $F_E + \Delta_2 F$.

*This report has been published in substantially the same form in *J. Geophys. Res.* 66(12):4013-4026, December 1961.

†Also engaged at the High Altitude Observatory, University of Colorado, in a program of research sponsored by the National Bureau of Standards and the Air Force Geophysical Research Directorate.

By continuing this process, a series of values of the belt field $\Delta_n F$ and of the combined field F_n are obtained:

$$F_n = F_E + \Delta_n F. \quad (3)$$

If F_n approaches a limiting value, this is expected to be the true field F given by Equation 1.

Akasofu and Chapman (Reference 4) have discussed the field $\Delta_1 F$ analytically for several model belts. They treated F_E as the field of a point dipole of vector moment M (8.31×10^{25} gauss cm³) situated at a point O inside the earth (centered or eccentric). In this case the belt and its field ΔF , hence the total field F , have symmetry about the dipole axis and equatorial plane. Also they made numerical calculations of several properties for a particular assumed model belt called V_3 , including the intensity $\Delta_1 H$ of the field $\Delta_1 F$, for points in the equatorial plane of the dipole M . The results obtained were compared with the Explorer VI (1959 δ) magnetic observations (Reference 5).

Their model belt involves a parameter $n_0 E$ which, for the same distribution of the belt, determined its density everywhere. The field $\Delta_1 F$ involves $n_0 E$ as a factor; that is, its intensity everywhere is proportional to $n_0 E$. For the particular value $n_0 E = 150$ the calculated field F_1 seemed to resemble the field observed by the satellite Explorer VI in the region up to about $7a$ (where $a = 6.37 \times 10^8$ cm is the earth's radius). However, in the region between $5a$ and $7a$, the observed field showed a notable proportionate departure from the earth's field F_E . Hence the calculated field $\Delta_1 F$ may not be a good approximation to the actual field ΔF of the belt. Akasofu and Chapman (Reference 4) stated that "further work on this problem is necessary to obtain a self-consistent system of current and field."

In this paper their numerical calculations for the model belt V_3 are extended to show the general character of the field $\Delta_1 F$ in the whole space around the earth. These results are compared with the changes observed at the earth's surface during magnetic storms. Also, the second approximation $\Delta_2 F$ to the field of this model belt has been calculated, for $n_0 E = 90$, in a region that includes the densest part of the belt. The difference between $\Delta_1 F$ and $\Delta_2 F$ suggests that, for this value of $n_0 E$, the field $\Delta_2 F$ is a good approximation to ΔF .

This problem is being explored further, particularly by calculating the potential of ΔF (or at least of $\Delta_1 F$) in terms of zonal harmonic functions. Alternative values of the belt radius and thickness, and also of a parameter of the pitch angle distribution are being considered.

GEOMETRICAL CONSIDERATIONS

The point O at which the dipole M is located is taken as the origin of coordinate systems r, θ, λ and x, z, λ , relative to a polar axis Oz antiparallel to M ; z is measured parallel and x perpendicular to Oz ; λ increases eastward, z northward. In a magnetic field which, like

F_e and F , is symmetrical with respect to Oz and the equatorial plane $z = 0$, it is convenient to substitute, for the coordinates r, θ of any point P , the parameters r_e, s_1 , where r_e denotes the distance from O to the point P_e (where the line of force through P crosses the plane $z = 0$) and s_1 denotes the length of the line of force from P_e to P (positive northward). Let h, j, k denote a right-handed orthogonal triad of unit vectors, with origin at P , h being the direction of H at P , and k along the eastward normal to the meridian plane through P ; $j = k \times h$. An element of length ds drawn from P is

$$ds = h ds_1 + j h_2 dr_e + k h_3 d\lambda. \quad (4)$$

Areal elements at P normal to h, j, k may be denoted by dS_1, dS_2, dS_3 :

$$\begin{aligned} dS_1 &= h_2 h_3 dr_e d\lambda, \\ dS_2 &= h_3 ds_1 d\lambda, \\ dS_3 &= h_2 dr_e ds_1. \end{aligned} \quad (5)$$

Let H_e, H denote the (scalar) magnetic intensities at P_e and P . The constancy of the strength $H dS_1$ of a tube of magnetic force along its length gives the relation

$$\left. \begin{aligned} h_2 &= \frac{r_e H_e}{h_3 H}, \\ h_3 &= r \sin \theta. \end{aligned} \right\} \quad (6)$$

Akasofu and Chapman (Reference 4) gave the special forms of h_2, r_e, H, H_e , and the radius of curvature R_c of the line of force at P , for the field F_e of the dipole M , in terms of r and θ . These factors are used in evaluating $\Delta_1 F$. In their Equation 4 $h_1 d\phi (= -h_1 d\theta)$ was used instead of ds_1 , where ϕ denoted the geomagnetic latitude.

In addition to the general relations of Equations 4 to 6 we also note that

$$\nabla = h \frac{\partial}{\partial s_1} + j \frac{\partial}{h_2 \partial r_e} + k \frac{\partial}{h_3 \partial \lambda}, \quad (7)$$

and

$$H \times (H \cdot \nabla) H = \frac{-H^3 j}{R_c}. \quad (8)$$

Equation 8 refers to a field like F , symmetrical about Oz , whose lines of force lie in meridian half-planes.

THE MODEL RADIATION BELT

The belt can be specified at each point P (with position vector \mathbf{r} relative to O) by the function $n(\mathbf{r}, \mathbf{w})$ expressing the distribution of particle velocities \mathbf{w} . There is such a function for each kind of particle in the belt; $n(\mathbf{r}, \mathbf{w}) d\mathbf{w}$ denotes the number density of these particles, at \mathbf{r} , whose velocities lie in the small range $d\mathbf{w}$ about the value \mathbf{w} . By symmetry, n is a function of s_1 , r_e , and w ; hence it can be written $n(s_1, r_e, w)$.

The angle between \mathbf{w} and \mathbf{H} at P is called the pitch angle ϕ . The distribution of the azimuth of \mathbf{w} around \mathbf{H} is isotropic except possibly at singular points of the field F . Hence, for the particles of this velocity group, the velocity distribution depends only on ϕ . It may be specified by a function $F(\phi)$ such that $F(\phi) d\phi$ denotes the fraction of all the particles of this group whose pitch angles lie between ϕ and $\phi + d\phi$. Thus

$$\int_0^\pi F(\phi) d\phi = 1 ; \quad (9)$$

and the number density at P of the particles (of any particular kind) with speeds between w and $w + dw$ can be denoted by $n(s_1, r_e, w) dw$. Clearly

$$\begin{aligned} \int n(\mathbf{r}, \mathbf{w}) d\mathbf{w} &= 2\pi \int \int n(s_1, r_e, w) F(\phi) w^2 dw d\phi \\ &= 2\pi \int n(s_1, r_e, w) w^2 dw . \end{aligned} \quad (10)$$

In general, as the particles move in the field F , their pitch angle distribution and number density vary from point to point. Parker (Reference 6) showed that the pitch angle distribution given by

$$F(\phi) = A(\alpha) \sin^{\alpha+1} \phi , \quad (11)$$

where

$$A(\alpha) = \frac{\Gamma(\alpha + 2)}{2^{\alpha+1} \left[\Gamma\left(\frac{\alpha}{2} + 1\right) \right]^2} ,$$

which satisfies Equation 9, has the following remarkable properties:

1. If $F(\phi)$ has this form at one point along a tube of force, this is its form for the same value of α all along this tube; and

2. The number density varies as $H^{-\alpha/2}$ along the tube, and we may write

$$n(s_1, r_e, w) = n(r_e, w) \left(\frac{H_e}{H} \right)^{\alpha/2} \quad (12)$$

where $n(r_e, w) dw$ denotes the number density at P_e of the particles with speeds between w and $w + dw$. Clearly the functional symbol n in Equation 12 has different meanings in the two cases.

Following Akasofu and Chapman (Reference 4) we consider a model belt in which $F(\phi)$ has the form of Equation 11, with the same value α throughout the whole field. Further, the density distribution in the equatorial plane $z = 0$ is

$$n(r_e, w) = n_0(w) \exp \left[-q^2 (r_e - r_{e0})^2 \right]. \quad (13)$$

Thus in this plane the radial distribution of the density is Gaussian for each particle speed. The factor q determines the radial spread of the belt. Conceivably q might be a function of w , but in this paper we consider only particles of a particular speed w or speed range w to $w + dw$; thus the results should be integrated with respect to w if the distribution functions of the speed w (or energy $E = 1/2 mw^2$) are known for the particles present.

The model belt of Reference 4 is specified here by Equations 11 and 13 with

$$\left. \begin{aligned} r_{e0} &= 6a, \\ \alpha &= -\frac{1}{2}, \\ \frac{q}{a} &= 1.517. \end{aligned} \right\} \quad (14)$$

These parameters are chosen merely to illustrate the numerical computation, and the same procedure can be applied to any set of parameters. In this case, the dipole line of force that crosses the plane $z = 0$ at $6a$ meets the earth's surface in geomagnetic colatitude $\theta = 24^\circ$. The choice $6a$ for r_{e0} , the radius of the center line of the belt distribution, is made because aurorae often appear during moderate magnetic storms at about that colatitude. The value $\alpha = -1/2$ corresponds to a pitch angle distribution that has more small pitch angles than would correspond to an isotropic distribution of the direction of w . The chosen value of q corresponds to a reduction of density to a tenth of the maximum value (also denoted by $n_0(w) dw$ or simply by n_0), at a radial distance a on either side of the center line of the belt, that is, at $5a$ and $7a$.

THE CURRENT DISTRIBUTION CORRESPONDING TO $\Delta_1 F$

Let i denote the contribution to the equivalent electric current intensity in the belt due to particles of any one kind with speeds between w and $w + dw$. Let i_1 denote the current intensity for the first approximation. Following Parker (Reference 6), Akasofu and Chapman expressed i_1 for a belt with the pitch angle distribution of Equation 11 substantially as follows (Reference 4, Equation 51):

$$i_1 = \frac{mcw^2 dw}{H} \left(\frac{H_e}{H} \right)^{\alpha/2} \left\{ n(r_e, w) \frac{[1 - 6B(\alpha)]}{P_c} - \frac{dn(r_e, w)}{dr_e} \frac{2R(\alpha)}{h_2} \right\}, \quad (15)$$

where

$$B(\alpha) = \frac{(\alpha + 2)}{4(\alpha + 3)}. \quad (16)$$

Equation 15 is valid for the general field F , where the current flows symmetrically round the axis Oz ; such a current distribution is called a ring current.

Akasofu and Chapman calculated the distribution of i for the model belt specified in Reference 4, section 3* when the total field present is taken to be the dipole field F_E . In this case their i will be denoted by i_1 ; then at any point P_0 on the center line of the belt ($z = 0$, $r_e = r_{e0}$), the value of i_1 is denoted by

$$\left. \begin{aligned} i_{10} &= 1.56 \times 10^3 mw^2 n_0(w) dw \text{ esu} \\ &= 1.66 \times 10^{-15} n_0(w) E dw \text{ amperes} , \end{aligned} \right\} \quad (17)$$

where E is the kinetic energy of the particle expressed in kev,

$$E = 3.12 \times 10^8 mw^2. \quad (18)$$

Akasofu and Chapman (Reference 4, Figure 3c) illustrated the current distribution by a set of current isolines, for the current intensities $i_1/i_{10} = 12, 10, 8, 6, 4, 2, -2, -4, -6$. Some of these lines ($10, \pm 6, \pm 2$) are reproduced here in Figure 1; the positive values correspond to westward current, negative to eastward, and the eastward isolines are dashed lines in the Figure. (Their Figure 3c shows by dot-and-dash lines the dipole lines of force through the points $r_e = 5a, 6a, 7a$.) The current intensity changes sign near P_0 ; slightly

*Note that a factor $(1 + \sin^2 \phi)$ should be added on the right of their Equation 53, that a factor $\cos \phi$ is omitted from Equation 29, and that in Equation 51 the index of the factor H_e/H should be $\alpha/2$. The numerical factor 1.66×10^{-15} in Equation 17 was written as 1.61×10^{-15} . These are errors only in the reproduction of the original text; the calculations were made from the correct formulas.

nearer to 0; the maximum westward and eastward current intensities slightly exceed $12 i_{10}$ and $6 i_{10}$. Also they illustrated separately (Figures 3a, 3b) the distribution of parts of i given in Equation 15; the distribution of the parts of i that are contributed by the diamagnetism and drift currents of the belt were to be shown later. The main contribution to the field comes from the diamagnetism.

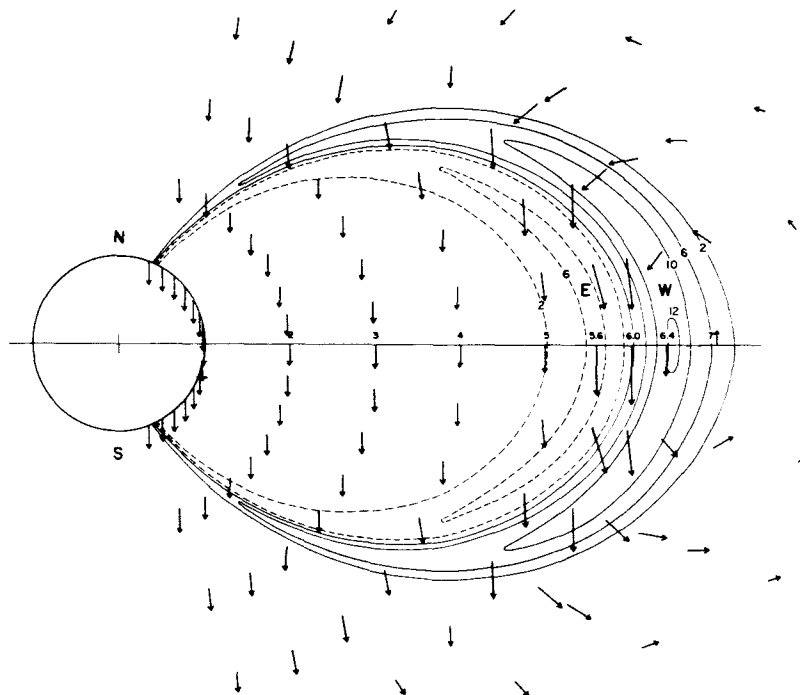


Figure 1—The field vectors of $\Delta_1 F$, the first approximation to the magnetic field of the model belt, in a meridian plane; and isolines of the equivalent current intensity in the belt (solid lines indicate westward, dashed lines eastward current). The vector scale of force, and the unit in which the current intensity is expressed, are proportional to the energy density $n_0 E$ (kev/cm³) at the center line of the belt, at 6 earth radii from the earth's center.

THE MAGNETIC FIELD $\Delta_1 F$

Akasofu and Chapman gave expressions (Reference 4, Equations 76 and 77) for the x and z components of the field $\Delta_1 F$, and calculated $\Delta_1 H_z$ numerically for points in the equatorial plane $z = 0$, where $\Delta_1 H_x = 0$ (see their Figure 6). Using the same formulas, and calculated values of i_1 at a network of points P in a meridian half-plane, the present authors evaluated $\Delta_1 H_x$ and $\Delta_1 H_z$ at a large number of points P' in this half-plane. Figure 1 shows some of the results by the vectors $\Delta_1 H$ for the points P' disposed along radii in latitudes

ϕ_1 from 0° to 70° at 10° intervals, mainly at intervals (a) of radial distance. Figure 2 illustrates these and other results in a different way. The lower portions of the figures are graphs of the x and z components of the $\Delta_1 F$ field on a linear scale along radii in latitude ϕ_1 from 0° to 50° , up to $r = 8a$, for a model belt such that $n_0 E = 150$, where

$$n_0 = n_0(w) dw \quad (19)$$

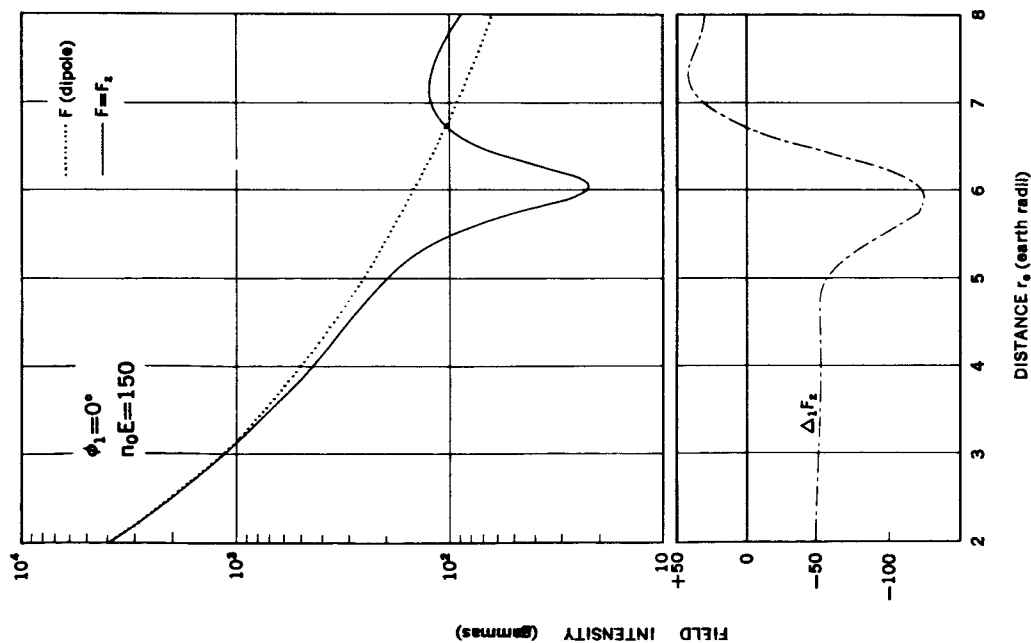
This might correspond, for example, to a maximum number density $1.5/\text{cm}^3$ of 100-kev particles, or $1/\text{cm}^3$ of 150-kev particles, at points P_0 on the center line of the belt. The upper parts of Figure 2 are graphs, on a logarithmic scale, of the intensity of the dipole fields F_E and F_1 . Figures 2b and 2c (upper) also show graphs of the x and z components of the field F_1 .

For this value of $n_0 E$ it is clear from Figure 2 that in certain regions, mainly near the center line of the belt, $\Delta_1 F/F_E$ is not small. Hence for this belt intensity it is inadequate to ignore the distortion of the field F_E by $\Delta_1 F$. However the graphs in the lower parts of these figures are valid for smaller values of $n_0 E$, with scales of force reduced proportionately.

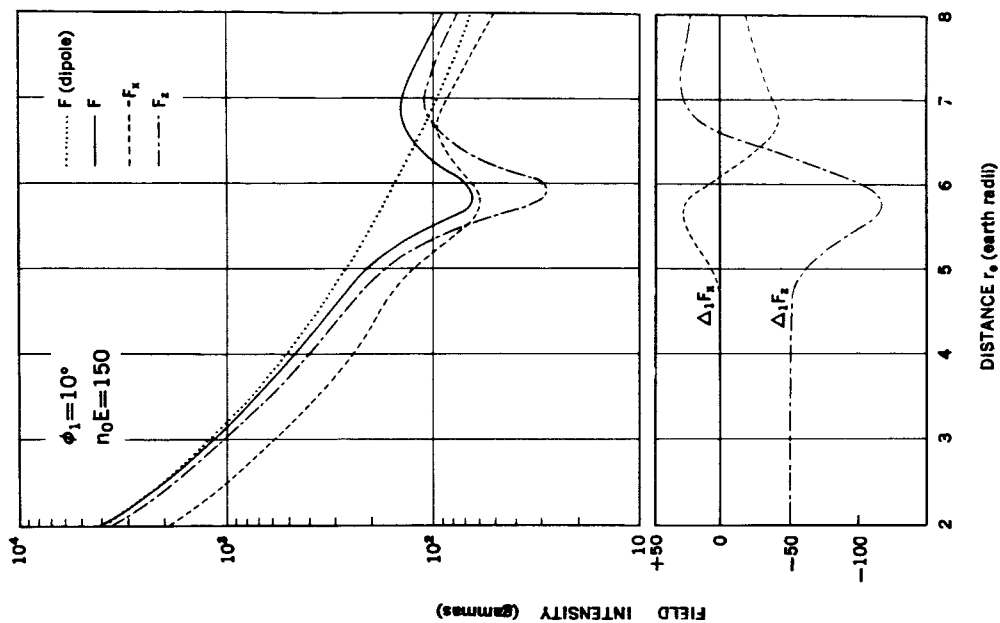
Figures 1 and 2a also indicate that within a radius of about $2a$ the field $\Delta_1 F$ is nearly uniform. Beyond this $\Delta_1 F$ becomes notably nonuniform, and shows considerable curl in the region of most intense current, centered about $6.5a$ in the equatorial plane. The field differs considerably from that of a toroidal current. Outside the belt the field $\Delta_1 F$ tends, with increasing distance, to similarity with the dipole field, as general theory would indicate.

Figure 2 may be useful for comparing the theory of the field of the model belt here considered with observations of the actual magnetic field around the earth. Clearly the greatest magnetic influence of the belt should be explored by satellites moving nearly in the equatorial plane. For comparison with satellite magnetic observations, tables of $\Delta_1 F$ have been calculated for many more points than are illustrated in the figures of this paper.

Figures 3 and 4 show some lines of force of the combined field $F_1 = F_E + \Delta_1 F$. These lines were calculated approximately, taking steps of length $0.1a$, for the values $n_0 E = 90$, 150. These lines correspond, for example, to distributions of 150-kev particles, of maximum number densities $1/\text{cm}^3$ and $0.6/\text{cm}^3$. Figures 3 and 4 show typical lines of force of the fields F_1 (solid lines) and F_E (dashed lines). The distortion of the F_1 lines is much greater for $n_0 E = 150$ than for $n_0 E = 90$. Within the center line of the belt, the ring current reduces the magnetic flux across the equatorial plane. Outside this line the flux is increased by an amount depending on the magnetic moment of the belt. Akasofu and Chapman gave a general formula for the magnetic moment of a belt of the type here considered (see Reference 4, section 4.4).

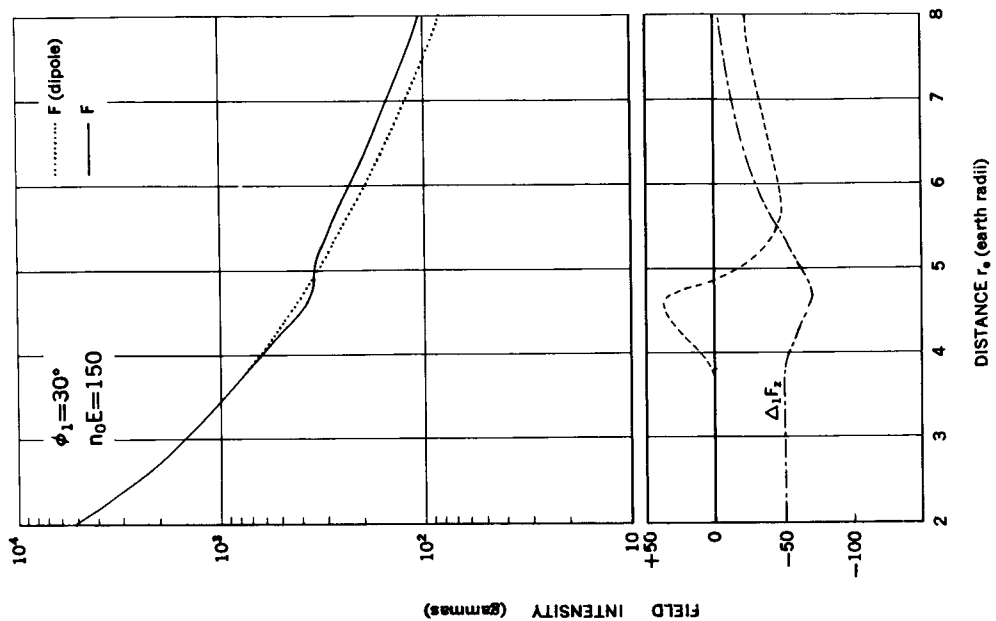


(a)

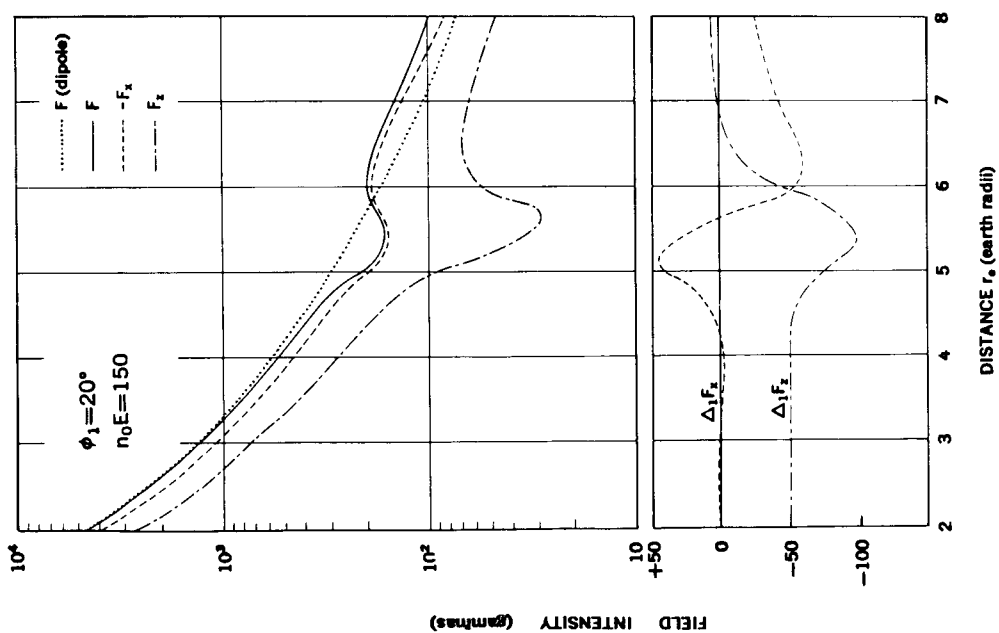


(b)

Figure 2—The first approximation to the distortion of the dipole field for the model belt centered at 6 earth radii for points lying along surfaces of constant latitude ϕ . The top half of the graphs give the resulting total field on a logarithmic scale; the lower portions give the disturbance vectors in the x and z directions.



(d)



(c)

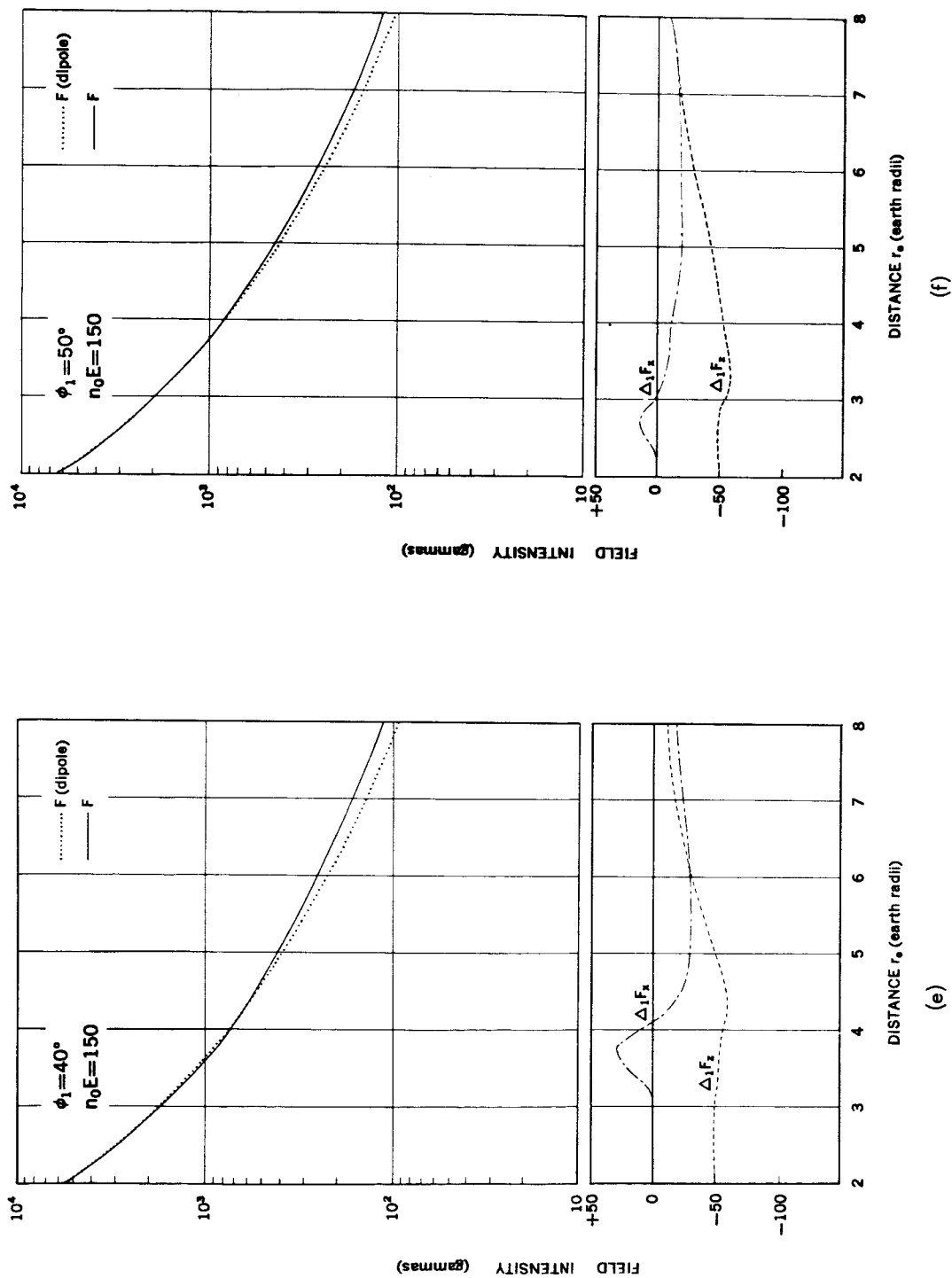


Figure 2 Cont. - The first approximation to the distortion of the dipole field for the model belt centered at 6 earth radii for points lying along surfaces of constant latitude ϕ . The top half of the graphs give the resulting total field on a logarithmic scale; the lower portions give the disturbance vectors in the x and z directions.

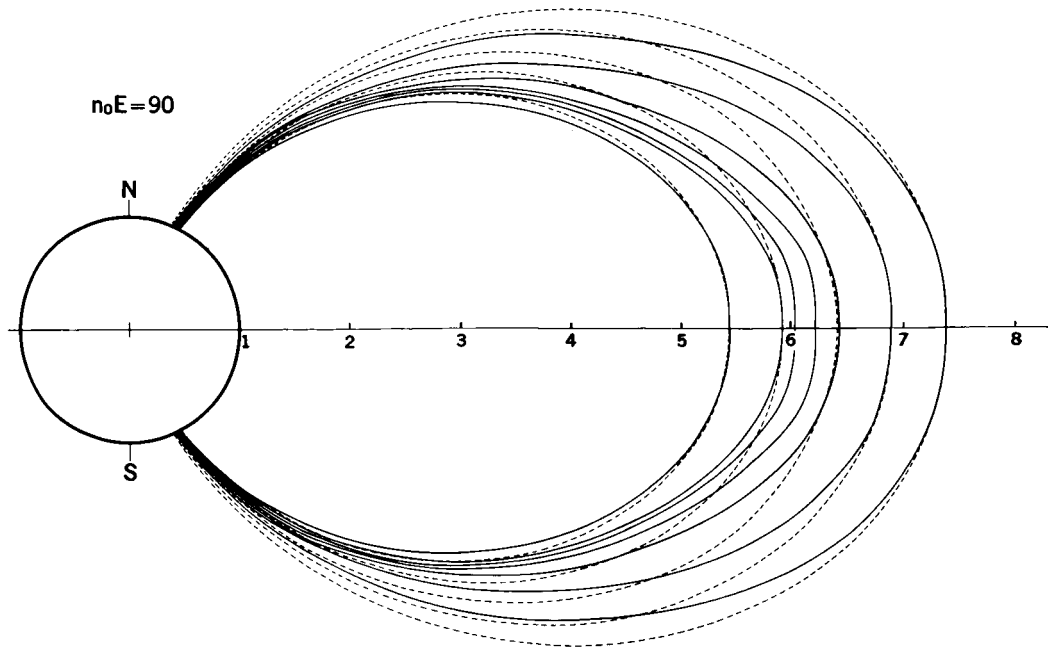


Figure 3—The lines of force of F_1 , the first approximation to the combined field of the geomagnetic dipole and the belt. The dashed lines are lines of force of the dipole field.

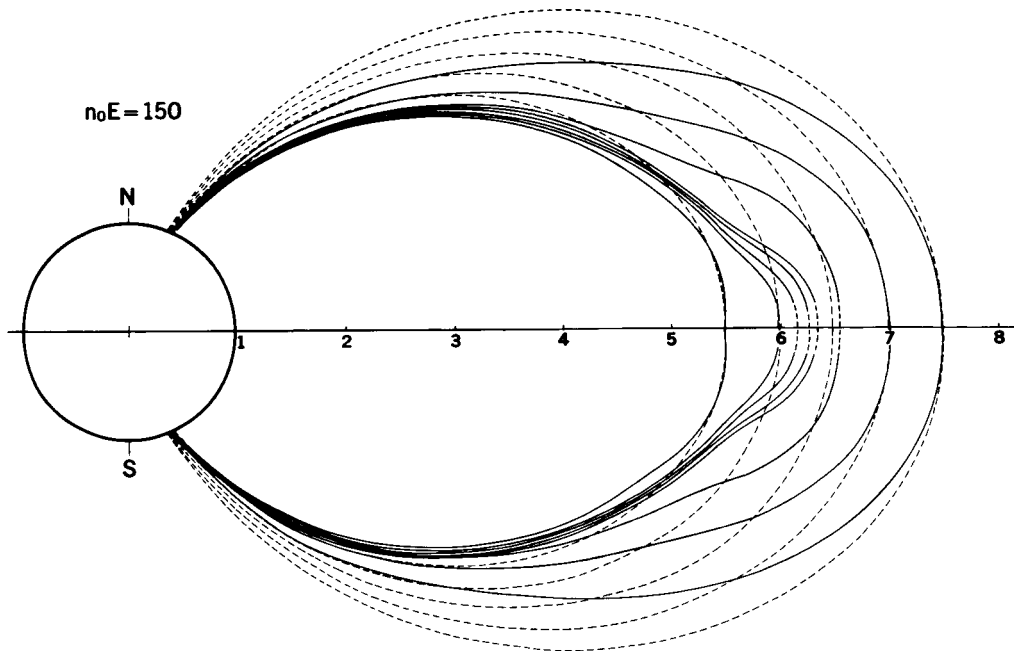


Figure 4—The lines of force of F_1 , the first approximation to the combined field of the geomagnetic dipole and the belt. The dashed lines are lines of force of the dipole field.

THE RING-CURRENT MAGNETIC DISTURBANCE OF THE EARTH'S SURFACE FIELD

The ring-current field at the earth's surface is nearly uniform and in the direction of M , the dipole moment, as is shown particularly by Figures 1 and 2a. Thus it decreases the horizontal component of the field and increases the numerical intensity of the vertical component. Changes in the field are observed during the main phase of magnetic storms. As the ring-current grows during the early hours of the storm, its changing field induces electric currents within the earth. They increase the change in the horizontal component and reduce that of the vertical component.

In Figure 5 the ring-current change of the horizontal component (denoted by H) at the earth's surface, is given as a function of latitude up to 70° , for $n_0 E = 150$. On the scale shown, the curve is indistinguishable from a sine curve corresponding to a uniform field suggested by Figure 1. The diagram also shows the graph of the vertical component V of the ring-current field at the earth's surface for $n_0 E = 150$. The curve is almost indistinguishable from the cosine curve corresponding to the sine curve for H , except near 65° latitude.

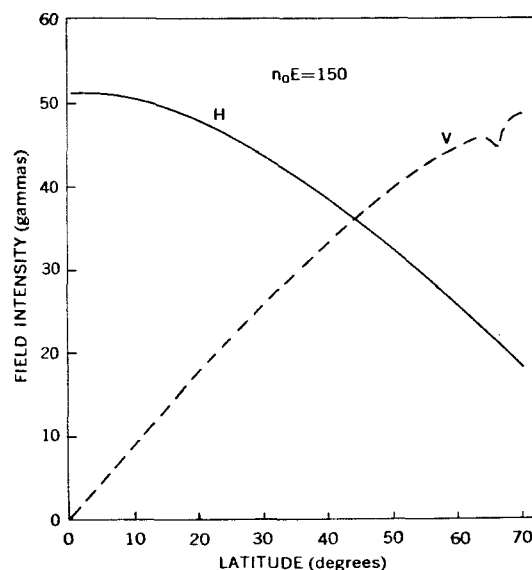


Figure 5—The variations of the horizontal and vertical components (H, V) of the field of the belt, at the earth's surface, from the equator to latitude 70° , to the first approximation for $n_0 E = 150$

However, calculations of the field components of ΔF were made for many points within and near the ring-current distribution (Figure 1), and they revealed a small irregularity of the field F in the current region, extending even to the earth's surface. This is to be attributed mainly to the diamagnetism of the belt. Figure 6 illustrates this feature in closer detail. It shows the variations of the total intensity $\Delta_1 F$, and of its horizontal and vertical components H and V at the earth's surface, between latitudes 58° and 70° . The irregularity affects V most, but its magnitude for $n_0 E = 150$ does not exceed 5 gammas (Reference 7, p. 2250). This model belt would reduce the earth's horizontal magnetic intensity at the equator by about 50 gammas; the induced earth currents would increase this to about 90 gammas (and would decrease the change in the vertical component). The irregularity of the vertical component in the auroral zone will not exceed 35 gammas. The *observed* decrease of the horizontal component at the maximum phase of the greatest magnetic storms

is of the order of 600 gammas. The actual changes in the vertical component are often as great as 1000 gammas, and sometimes much more. In those latitudes the field of the belt, mainly diamagnetic, is insignificant by comparison, as was recognized by Dessler and Parker (Reference 7). This conclusion contrasts with the diamagnetic explanation of polar magnetic disturbance suggested long ago by Hulburt (Reference 8) and criticized by Chapman (Reference 9, section 10).

THE SECOND APPROXIMATION ($\Delta_2 F$) TO THE FIELD OF THE RING CURRENT

For the values of $n_0 E$ considered in the two preceding sections the field of the ring current materially modified the dipole field in the regions of greatest current intensity. Hence our calculation of $\Delta_1 F$, the first approximation to the ring-current field, needs correction for comparison with observed magnetic changes during storms.

The current intensity has been recalculated at a network of points $P_{m,n}$ (Figure 7), for the model belt specified by Equations 11, 13, and 14, in the presence of the field $F_1 = F_E + \Delta_1 F$. This calculation has been made for the case $n_0 E = 90$. The point $P_{m,n}$ lies on the line of force for which $r_e = 4.8a + m \times 0.1a$ and is at the distance s_1 along this line from the plane $z = 0$; s_1 is given by $s_1 = 0.1a + n \times 0.2a$. The values of m ranged from 0 to 27 (i.e., 28 lines of force), and the values of n ranged from 0 to 27 for $m = 0$ and from 0 to 45 for $m = 27$.

The calculated current intensity at $P_{m,n}$ is denoted by $(i_2)_{m,n}$, where the subscript

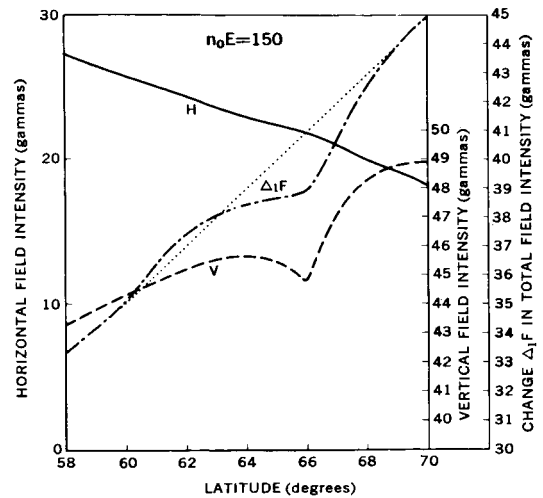


Figure 6—Enlarged version, for the latitude range 58° to 70° (near the tip of the model belt), of the H and V curves of Figure 5; and the variation of $\Delta_1 F$, the corresponding total vector $\sqrt{H^2 + V^2}$ (the dotted line shows the interpolated curve for $\Delta_1 F$, to indicate the slight irregularity due to the belt). Note the three different scales for H, V, and $\Delta_1 F$.

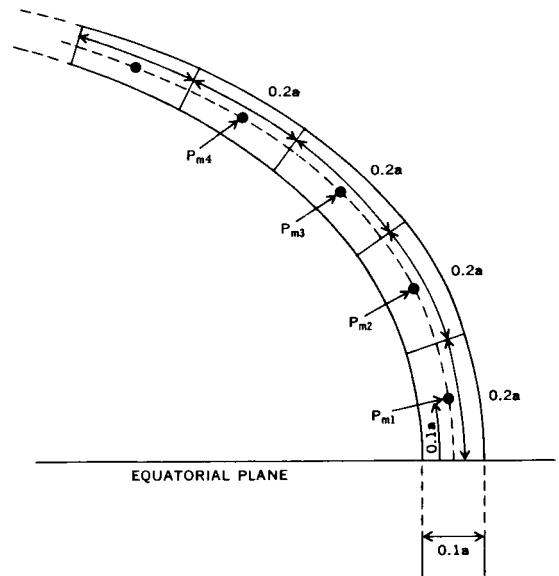


Figure 7—The subdivision of the meridian plane used in computing $\Delta_2 F$, the second approximation to the field of the belt; the curved lines are lines of force of the field F_1 (see Figures 3 and 4).

2 indicates that the value is a second approximation to i , corresponding to motion of the particles in the field F_1 . The values of i_2 were calculated from Equation 15, using the values of H , h_2 , R_c numerically computed for the field F_1 and its lines of force.

The values of i_2 at the points $P_{m,n}$ having been obtained, the magnetic field $\Delta_2 F$ was computed at another network of points $P'_{m,n}$, by using formulas 76 and 77 of Reference 4. The current distribution was divided into filaments (Figure 7) centered at the point $P_{m,n}$ and of cross sections $h_2 dr_e ds_1$; the value $(i_2)_{m,n}$ was taken to represent the mean current over this section. The number of points $P_{m,n}$ in the two (northern and southern) halves of the meridian section of the belt exceeded 2000. The field $\Delta_2 F$ was computed for points $P'_{m,n}$ along radii in latitudes $\phi_1 = 0^\circ, 10^\circ, 20^\circ$, at radial distances a to $8a$. The radial interval was $0.2a$ from $r_e = 4.4a$ to $r_e = 7.6a$. These results are embodied in numerical tables (not reproduced here).

Figure 8 illustrates the variation of $\Delta_2 F$ and F_2 in the equatorial plane in the same manner as Figure 2a does for $\Delta_1 F$ and F_1 ; Figure 2 refers to $n_0 E = 150$, and Figure 8 to $n_0 E = 90$. The second approximation corrects $\Delta_1 F$ in this plane by a maximum amount of 15 gammas, at a point near P_0 . The change from $\Delta_1 F$ to $\Delta_2 F$ scarcely alters the location (just within the center line of the belt) where $\Delta_1 F$ is most intense, but it deepens this minimum by about 15 gammas, from 75 to 90. Except in this region, which produces a minimum of F_1 and F_2 near P_0 , the second approximation makes a correction of less than 10 gammas; and at the earth's surface the correction does not exceed 3 gammas. It seems likely that further approximations would produce little additional correction, so that $\Delta_2 F$ and F_2 nearly equal ΔF and F .

The dip in the fields F_1 and F_2 between $5a$ and $7a$ is shown on a linear scale by an inset in Figure 8.

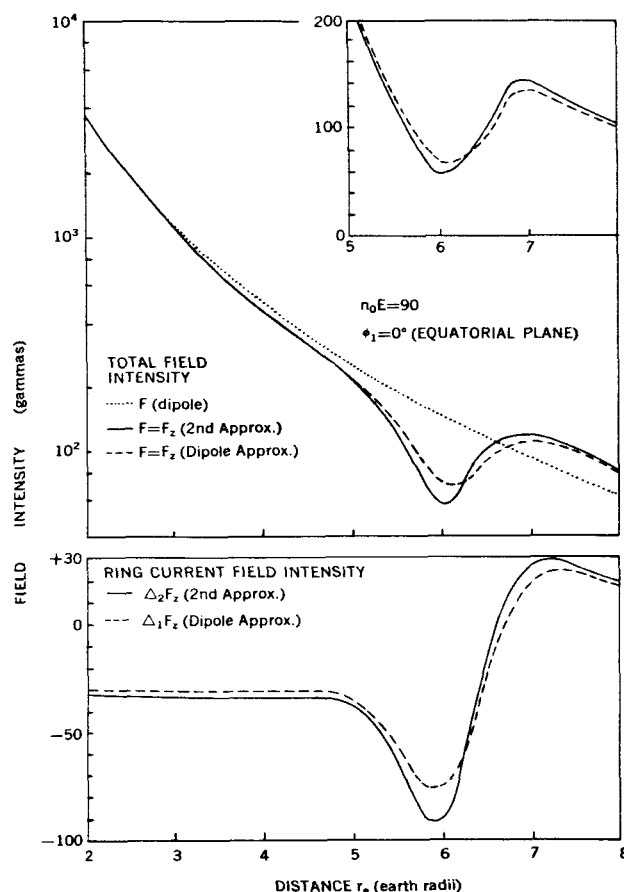


Figure 8—Similar to Figure 2, but for $n_0 E = 90$, and with the addition of the second approximation to ΔF (below) and to the combined field F (above). The broken line gives the first approximation, the solid line the second. Top right: the variation of F_1 (broken line) and F_2 (solid line) on a linear scale, between $5a$ and $7a$.

Near the center line of the belt, for $n_0E = 90$, the estimated intensity of the true field F in the equatorial plane will be reduced to about 55 gammas.

For $n_0E = 150$, the first approximation to the combined field is shown in Figure 2a; it reaches a minimum value of about 24 gammas. Because in the second approximation, the minimum value is smaller than that for the first approximation, it may be expected that the above value of 24 gammas also becomes smaller.

If n_0E is great enough to reduce the field F to a low value near P_0 , the guiding center approximation (Reference 10) used in obtaining Equation 15, may cease to be valid near P_0 . The paths of the particles there would be extremely complicated and the current intensity calculation must be modified. However, the dip near P_0 is mainly produced by the strong eastward current and the westward current, centered respectively at about 5.5a and 6.5a, where ΔF is relatively small and where the guiding center approximation will remain approximately valid.

In order to demonstrate this, Δ_2F was recalculated for $n_0E = 90$, neglecting the contribution from the current in a region around P_0 , limited by the lines of force $r_e = 5.9a$ and $r_e = 6.1a$, and by the radii between latitudes $\pm 10^\circ$. At 6a, the value of Δ_2F thus calculated was found to be 83.9 gammas; this may be compared with $\Delta_2F = 90.1$ gammas for the complete belt. Thus, more than 90 percent of the field decrease near P_0 is produced by the particles outside the above limits.

There is some doubt about what will happen if the value of n_0E is further increased. Beyond a certain value of n_0E the field *may* be reversed near P_0 . It is interesting to note that such reversals have been observed in the thermonuclear reaction vessels (mirror machines) in which a very hot plasma is confined by a strong magnetic field (Reference 11). Akasofu and Chapman (Reference 12) have attributed much importance to such a reversal in the formation of auroras.

THE RING-CURRENT FIELD BEYOND THE BELT

Akasofu and Chapman calculated the first approximation Δ_1M to the magnetic moment of the model belt considered here (Reference 4, section 4.4). Their value was $1.17 \times 10^{23} n_0E$ gauss cm^3 . Hence the equatorial field intensity F_1 beyond the belt will tend asymptotically with increasing distance to the value $(M + \Delta_1M)/r_e^3$. Table 1 gives the values of M/r_e^3 , $(M + \Delta_1M)/r_e^3$, and the calculated values of F_1 , from 8a to 15a at intervals of a for the case $n_0E = 150$. The values are expressed in gammas. Table 1 shows that at 15a the field approximates closely that of a dipole $M + \Delta_1M$.

For $n_0E = 90$, equatorial values of F_2 have been calculated up to $r_e = 8a$. The values of F_1 and F_2 at 8a in this case are 80.0 and 81.7; at this distance $(M_1 + \Delta_1M)/r_e^3$ for $n_0E = 90$ is 70.4.

Table 1
The ring-current field beyond the belt

Magnetic Parameter	Calculated Value* (gammas)							
	$r_e = 8a$	$r_e = 9a$	$r_e = 10a$	$r_e = 11a$	$r_e = 12a$	$r_e = 13a$	$r_e = 14a$	$r_e = 15a$
M/r_e^3	62.5	43.9	32.0	24.0	18.5	14.6	11.7	9.5
$(M + \Delta_1 M)/r_e^3$	75.7	53.2	38.8	29.1	22.4	17.6	14.1	11.5
F_1	91.6	61.1	43.2	31.8	24.2	18.8	15.0	12.1

*Reference 4

THE NONSTEADY STATE

During a magnetic storm there are great changes in the number and distribution of the energetic particles in the region beyond the inner radiation belt. Akasofu and Chapman (Reference 4) have discussed these changes, as observed from satellites (Reference 13), in connection with the magnetic variations during particular storms.

The formulas used to determine the field of the ring current of a steady radiation belt do not suffice for a changing belt. The corresponding changes in the field F introduce an electric field E such that

$$\frac{\partial \mathbf{H}}{\partial t} = -\frac{1}{c} \text{curl } \mathbf{E}.$$

Assuming axial symmetry, and using cylindrical coordinates,

$$\frac{\partial H_z}{\partial t} = -\left(\frac{1}{cr}\right) \frac{\partial(rE_\lambda)}{\partial r}$$

for the electric intensity E_λ in the direction λ . This electric field adds a term \mathbf{v} equal to $(\mathbf{E} \times \mathbf{H})/cH^2$ or $E_\lambda \mathbf{j}/cH_z$ to the velocity of the particles, and a term $(nmc/H^2) \mathbf{H} \times d\mathbf{v}/dt$ to the current intensity i . The velocity \mathbf{v} is directed outward or inward, in the meridian plane; it tends to distort the density distribution. A complete discussion of the ring current must take account of this electric field and of various loss processes in the belt.

ADDENDUM

Further computations of the magnetic field have been made for measured particle distributions during quiet (Reference 14) and disturbed (Reference 15) magnetic conditions.

Computations have also been made (Reference 16) for different types of belts. Further discussion of the methods of calculation of the magnetic field of trapped particles is given in References 17 and 18.

REFERENCES

1. Van Allen, J. A., and Frank, L. A., "Radiation around the Earth to a Radial Distance of 107,400 km," *Nature* 183(4659):430-434, February 14, 1959
2. Vernov, S. N., Chudakov, A. E., Vakulov, P. A. and Logachev, Yu. I., "Study of Terrestrial Corpuscular Radiation and Cosmic Rays during Flight of the Cosmic Rocket," *Doklady Akad. Nauk SSSR* 125(2):304-307, March 11, 1959; also Translation, *Soviet Phys. - Doklady* 4(2):338-342, October 1959
3. Singer, S. F., "A New Model of Magnetic Storms and Aurorae," *Trans. Amer. Geophys. Union*, 38(2):175-190, April 1957
4. Akasofu, S.-I., and Chapman, S., "The Ring Current, Geomagnetic Disturbance and the Van Allen Radiation Belts," *J. Geophys. Res.* 66(5):1321-1350, May 1961
5. Sonett, C. P., et al., "Current Systems in the Vestigial Geomagnetic Field: Explorer VI," *Phys. Rev. Letters* 4(4):161-163, February 15, 1960
6. Parker, E. N., "Newtonian Development of the Dynamical Properties of Ionized Gases of Low Density," *Phys. Rev.* 107(4):924-933, August 15, 1957
7. Dessler, A. J., and Parker, E. N., "Hydromagnetic Theory of Geomagnetic Storms," *J. Geophys. Res.* 64(12):2239-2252, December 1959
8. Hulburt, E. O. "On the Ultraviolet Light Theory of Aurorae and Magnetic Storms," *Phys. Rev.* 34(2):344-351, July 15, 1929
9. Chapman, S., "On Solar Ultra-Violet Radiation as the Cause of Aurorae and Magnetic Storms," *Monthly Notices Roy. Astron. Soc., Geophys. Suppl.* 2(6):296-300, March 1930
10. Alfvén, H., "Cosmical Electrodynamics," London: Oxford University Press, 1950
11. Green, T. S., "Evidence for the Containment of a Hot, Dense Plasma in a Theta Pinch," *Phys. Rev. Letters* 5(7):297-300, October 1, 1960
12. Akasofu, S. I., and Chapman, S., "A Neutral Line Discharge Theory of the Aurora Polaris," *Phil. Trans. Roy. Soc. London* 253A(1031):359-406, April 27, 1961
13. Arnoldy, R. L., Hoffman, R. A., and Winckler, J. R., "Observations of the Van Allen Radiation Regions during August and September 1959, Part 1," *J. Geophys. Res.* 65(5):1361-1376, May 1960
14. Akasofu, S.-I., Cain, J. C., and Chapman, S., "The Magnetic Field of the Quiet-Time Proton Belt," *J. Geophys. Res.* 67(7):2645-2647, July 1962

15. Akasofu, S.-I., and Cain, J. C., "A Model Storm-Time Proton Belt," Paper presented at the Forty-third Annual Meeting, American Geophysical Union, Washington, D. C., April 25-28, 1962
16. Akasofu, S.-I., and Cain, J. C., "The Magnetic Field of the Radiation Belts," *J. Geophys. Res.* 67(10):4078-4080, September 1962
17. Beard, D. B., "Self-Consistent Calculation of the Ring Current," *J. Geophys. Res.* 67(9):3615-3616, August 1962
18. Akasofu, S.-I., "On a Self-Consistent Calculation of the Ring Current Field," *J. Geophys. Res.* 67(9):3617-3618, August 1962